Design and Experimental Verification of the Drilling-While-Sampling Motor Control System for Geological Sampling

Liu Weidong

Xi'an Shiyou University, Xi'an, Shaanxi, 710000, China

Abstract: To meet the requirements of low-speed stability and circle count measurement for the high-temperature and strong-vibration while-drilling sampling actuator, a PMSM control system based on TMS320F28335 was developed. The system adopts FOC and introduces Mamdani fuzzy two-degree-of-freedom PI speed control to complete the 360×42 mm drive and control integrated board. A screw rod slide platform was built and verified by combining resolver counting and electronic scale displacement verification. The results show that the relative circle count steady-state error is 0.1228 circles (0.0106% FS), and the absolute cumulative error is 48.85 circles (0.3008% FS), meeting the ≤1% FS index.

Keywords: Stratigraphic sampling; Permanent magnet synchronous motor; Motor control

DOI: 10.62639/sspjinss07.20260301

1. Introduction

The rapid development of unconventional oil and gas resources has promoted the use of logging-while-drilling (LWD) formation-sampling tools. In harsh downhole environments involving high temperature, high pressure, and strong vibration, the actuator must maintain stable low-speed operation, and the lead-screw revolution count must be measured with high reliability. However, conventional PI control is susceptible to overshoot, and cumulative counting errors may occur during reversal[1]. To overcome these limitations, a PMSM field-oriented control (FOC) system based on the TMS320F28335 was established. A fuzzy two-degree-of-freedom PI controller was adopted, and a 360 × 42 mm integrated drive-and-control board was developed [2]. Turn-count tracking tests were performed on a lead-screw slide platform under no-load and 25 N·m conditions. Experimental results show that the system provides stable low-speed tracking, while the key measurement index remains within 1% FS.

2. Control System Design and Implementation

(1) Overall architecture of the control system

Based on technical index analysis, literature review, and theoretical analysis, the overall design block diagram of the permanent magnet synchronous motor control system for the logging-while-drilling formation sampling tool was developed, as shown in Fig. 1.

(Manuscript NO.: JINSS-26-1-62016)

About the Author

Liu Weidong (2001–), male, Han ethnicity, a native of Mudanjiang, Heilongjiang Province, Master of Engineering, School of Electronic Engineering, Xi'an Shiyou University. His research interests include motor control and electric drives.

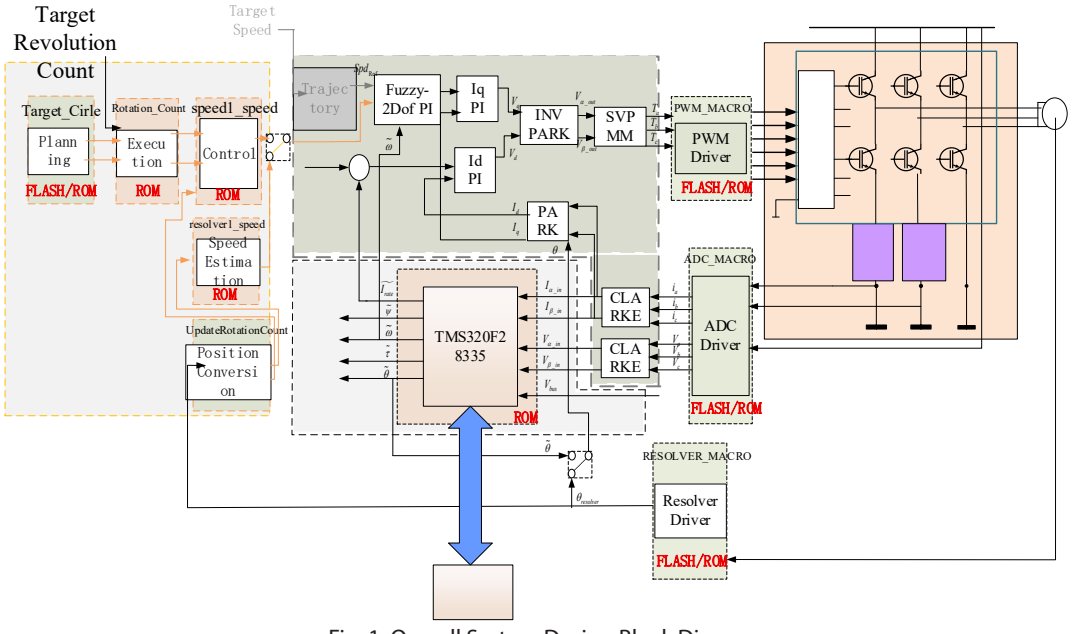

Fig. 1. Overall System Design Block Diagram

The overall architecture of the system is centered on the TMS320F28335 DSP. On the left side, the "target/control" unit generates the turn-count and speed commands, while the angular position and speed feedback signals from the resolver are decoded to form the outermost speed closed loop. Inside the DSP, a fuzzy two-degree-of-freedom PI controller is first introduced to improve low-speed response and disturbance rejection. In the speed loop, the reference speed $w*$ and the feedback speed w are used to construct the speed error e and its variation Δe, which are then taken as the two inputs of the fuzzy PI controller. The fuzzy rule base adopts a Mamdani inference structure, and the membership functions of the input variables are triangular. Each rule determines the fuzzy output according to the input error and its variation, and the representative value after rule inference is obtained. Finally, the output is defuzzified by the centroid method to generate a continuous control increment. Studies have shown that the combination of a Mamdani-type fuzzy controller and centroid defuzzification can produce smooth and continuous control actions, which is beneficial for accurate speed and position control. The software implementation flowchart of the speed controller is shown in Fig. 2.

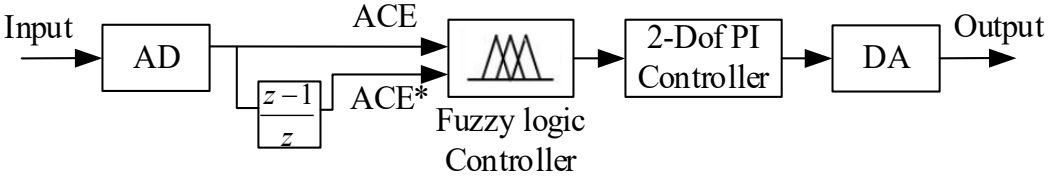

Fig. 2. Discrete Implementation Schematic of the Fuzzy Two-Degree-of-Freedom PI Speed Controller

(2) Fuzzy two-degree-of-freedom PI speed control strategy

The fuzzy controller designed in this study adopts a two-input single-output architecture, in which the inputs include the speed error eand its rate of change Δe(approximately obtained from the first-order difference of the error). These two variables jointly characterize the instantaneous deviation and its dynamic trend, thereby reproducing the coordinated regulation effect of the proportional and differential actions in a PI controller. The controller output is the speed adjustment increment Δu, which corresponds to a slight correction of the torque or q-axis current in the permanent magnet synchronous motor drive. The fuzzy inference module takes the speed error eand its rate of change Δe as inputs and outputs the PI parameters K_p and K_i. The speed adjustment increment Δuis then calculated by the incremental PI controller, and closed-loop speed regulation can be achieved through

successive accumulation, while the integral effect is naturally introduced to eliminate the steady-state error. The inference mechanism employs a Mamdani-type rule base, and the defuzzification process uses the centroid method, thereby generating continuous and accurate control commands.

In this design, the error *e* and its rate of change Δ*e* are divided into seven fuzzy subsets, namely NB, NM, NS, ZO, PS, PM, and PB. A symmetric triangular membership function is defined for each subset, uniformly covering the interval [−1,1], so that the error and its rate of change remain symmetrically distributed with respect to zero.

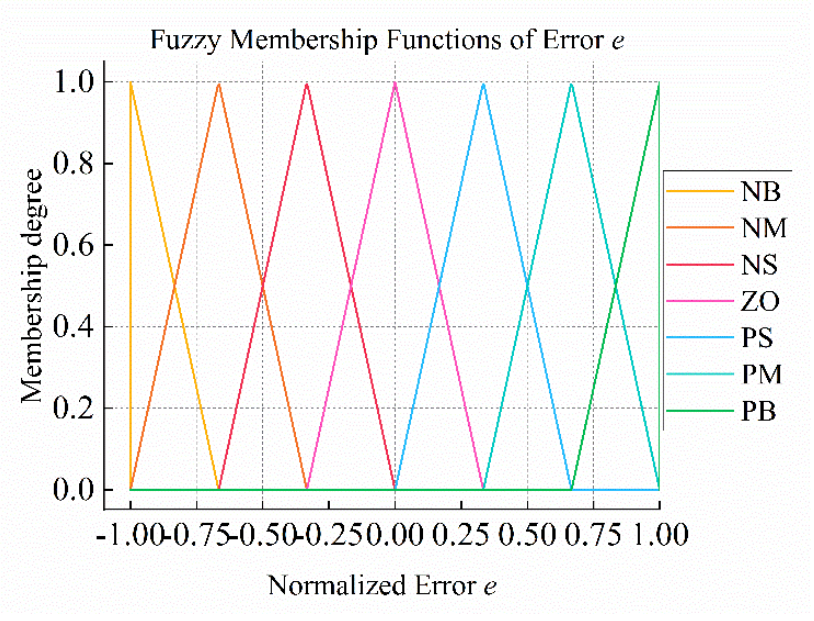

Fig. 3. Fuzzy Membership Functions of the Error e

Figure 3 shows the seven-level triangular membership distribution of the error *e* over the interval −1,1. The membership functions at each level are left-right symmetric and partially overlap with adjacent levels, which helps maintain sensitivity when the error approaches zero while avoiding abrupt switching in the large-deviation stage, thereby ensuring a smooth regulation process.

In this study, a fuzzy rule base was established by combining the control objectives with engineering experience, and the rules are expressed in the form of "condition–result" to represent the control strategy. When both the error and its rate of change are large, a relatively large control adjustment is generated. As the error decreases and its rate of change becomes smaller, the control action is gradually weakened to suppress overshoot. When the error approaches zero and is about to cross the zero point, a reverse or weakened action is applied in advance to accelerate convergence. Tables 1-1 and 1-2 list the adopted rule tables.

Table 1-1. Fuzzy Control Rule Table for K_p

e	Δ*e*						
	NB	NM	NS	ZO	PS	PM	PB
NB	PB	PB	PM	PM	PS	ZO	ZO
NM	PB	PB	PM	PS	PS	ZO	NS
NS	PM	PM	PM	PS	ZO	NS	NS
ZO	PM	PM	PS	ZO	NS	NM	NM
PS	PS	PS	ZO	NS	NS	NM	NM
PM	PS	ZO	NS	NM	NM	NM	NB
PB	ZO	ZO	NM	NM	NM	NB	NB

Table 1-2. Fuzzy Control Rule Table for K_i

e	Δe						
	NB	NM	NS	ZO	PS	PM	PB
NB	NB	NB	NM	NM	NS	ZO	ZO
NM	NB	NB	NM	NS	NS	ZO	ZO
NS	NB	NM	NS	NS	ZO	PS	PS
ZO	NM	NM	NS	ZO	PS	PM	PM
PS	NM	NS	ZO	PS	PS	NM	PB
PM	ZO	ZO	PS	PS	PM	PB	PB
PB	ZO	ZO	PS	PM	PM	PB	PB

The flowchart of the fuzzy control process is shown in Fig. 4. For the given input speed error e and error variation Δe, the membership degrees of the inputs with respect to each fuzzy set are obtained from the membership functions, denoted by $\mu_{E_i}(e)$ and $\mu_{\Delta E_j}(\Delta e)$. According to the obtained membership degrees and the fuzzy rule table, the firing strength of each rule is calculated $\alpha_{ij} = \min \mu_{E_i}(e), \mu_{\Delta E_j}(\Delta e)$

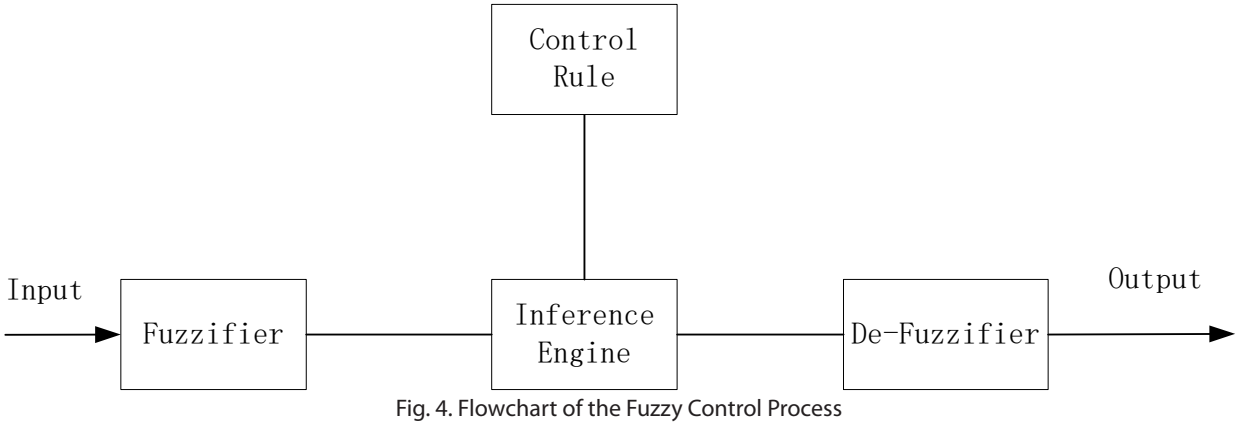

Fig. 4. Flowchart of the Fuzzy Control Process

In Mamdani inference, the firing strength of each rule is calculated according to the input membership degrees, and the representative values of the corresponding consequents, $K_{p,ij}$ and $K_{i,ij}$, are then obtained. The output section adopts the center-average (weighted-average) method to perform defuzzification, thereby yielding the online tuned parameters $K_p(k)$and $K_i(k)$.

The two-degree-of-freedom PI (Proportional–Integral) controller extends the conventional PI controller by introducing the capability to regulate the reference input channel and the feedback channel separately. In the conventional PI controller (single-degree-of-freedom), the control error is directly applied to the same PI loop, so it is impossible to distinguish errors caused by command changes from those caused by disturbances. By contrast, the two-degree-of-freedom PI controller introduces measures such as a setpoint weighting coefficient in the proportional path, so that the response to setpoint variations and the response to disturbances can be adjusted independently.

The control law of the two-degree-of-freedom PI controller can be expressed as Eq. (1-1).

$$u_{\mathrm{PI}}(t) = K_p\left[b\omega^*(t) - \omega(t)\right] + K_i\int_0^t\left[\omega^*(\tau) - \omega(\tau)\right]d\tau \quad (1\text{-}1)$$

Here, $\omega^*(t)$is the reference speed, $\omega(t)$is the actual speed, K_p and K_i are the proportional and integral gains, respectively, and b is the setpoint weighting coefficient. When b=1, the controller reduces to the conventional PI controller. As pointed out by Sitthisak[3], the two-degree-of-freedom PI controller enables separate tuning of tracking performance and disturbance rejection performance by weighting the reference signal and the feedback signal differently. Its structural block diagram is shown in Fig. 5.

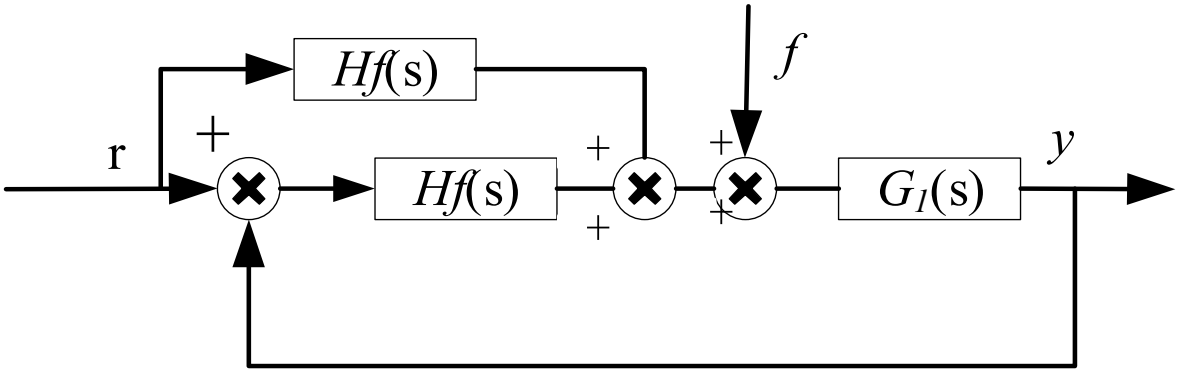

Fig. 5. Block Diagram of the 2DOF-PI Controller

The upper branch $H_f(s)$ acts only on the reference input to shape the transient response, whereas the lower branch $H_f(s)$ acts on the complete error signal to suppress external disturbances. Through proper tuning, faster setpoint tracking can be achieved without sacrificing robustness to load variations, thereby providing better overall performance than the single-degree-of-freedom PI controller.

Combined with the foregoing description, the speed two-degree-of-freedom PI controller can be represented in the form of either a transfer function or a state-space equation. If expressed in the Laplace domain, the transfer function of the 1DOF-PI controller is given by Eq. (1-2).

$$C_{\mathrm{PI}}(s) = K_p + K_i / s \quad (1\text{-}2)$$

After introducing the setpoint weighting coefficient b, the relationship between the equivalent input and output can be expressed as Eq. (1-3):

$$U(s) = K_p\left[b\Omega^*(s) - \Omega(s)\right] + \frac{K_i}{s}\left[\Omega^*(s) - \Omega(s)\right] \quad (1\text{-}3)$$

where $\Omega^*(s)$and $\Omega(s)$denote the Laplace transforms of the reference speed and the actual speed, respectively. Equation (1-3) reflects the operating principle of the two-degree-of-freedom controller. In this expression, the proportional term coefficient bacts on the reference signal, whereas the integral term acts on the overall error, thereby separating the regulation of the setpoint response from that of the disturbance response.

In the discrete-time implementation, the controller is usually described by a difference equation. For a system with sampling period T, the speed error $e[k]$ is given by Eq. (1-4):

$$e[k] = \omega^*[k] - \omega[k] \quad (1\text{-}4)$$

The PI control increment is expressed as Eq. (1-5):

$$\Delta u_{PI}[k] = K_p\left(b\left(\omega^*[k] - \omega^*[k-1]\right) - \left(\omega[k] - \omega[k-1]\right)\right) + K_i T\, e[k] \quad (1\text{-}5)$$

Equation (1-5) is equivalent to introducing the setpoint weighting coefficient binto the discrete PI controller.

Accordingly, the controller output is updated as Eq. (1-6):

$$u[k] = u[k-1] + \Delta u_{\mathrm{PI}}[k] \quad (1\text{-}6)$$

For fuzzy control, the essence is a nonlinear mapping, as shown in Eq. (1-7):

$$F : (e, \Delta e) \mapsto \Delta u \quad (1\text{-}7)$$

A strict analytical expression of the fuzzy two-degree-of-freedom PI controller can be given in a piecewise form. However, due to the large number of rules, it is commonly described by set representation or algorithmic procedures. Therefore, the fuzzy controller can be concisely represented in operator form as shown in Eq. (1-8):

$$\Delta u(k) = F\big(e(k), \Delta e(k)\big) \quad (1\text{-}8)$$

where F(·)represents the fuzzy rule inference and defuzzification process. The increment is accumulated to obtain the actual control input u(*k*). Since Fis a nonlinear piecewise function, the fuzzy two-degree-of-freedom PI controller can be regarded as a nonlinear extension of the conventional PI controller, with different gains and action strengths in different error intervals. For example, when the error eis large, the fuzzy controller exhibits a "high-gain" rapid correction effect; when the error eapproaches zero and the error variation Δeis small, it exhibits a "low-gain" slow convergence effect, thereby achieving an adaptive control law.

3. Experimental Platform and Test Methods

The experimental platform consists of three parts: the power supply and control unit, the load application unit, and the transmission actuator mechanism. The power supply section employs two DP831 DC power supplies to provide power for the control board and the magnetic powder brake, respectively. In addition, a separate DC power supply is used to supply the high-voltage DC bus. The load and transmission section consists of a magnetic powder brake, a reducer, a permanent magnet synchronous motor, a lead screw, and a cylinder set, which are used to realize rotational loading and reciprocating motion of the mechanism. The host computer communicates via RS-485 to issue control commands and record operating data.

To evaluate the operating performance of the designed control system under load conditions, emphasis was placed on the turn-count control accuracy and speed-tracking performance under load, so as to verify the control stability and execution accuracy of the system under loaded operation.

4. Experimental Results and Analysis

The turn-count command is applied in a reciprocating manner along a preset trajectory between 0 and 1160 turns, while the variations of the reference turn count and the actual turn count with time are recorded simultaneously to reflect the tracking lag and accumulated error under long-stroke reciprocating conditions.

At the full-stroke target position, the actual turn count is 1160.1228 turns, with a steady-state deviation of 0.1228 turns, corresponding to an error of 0.0106%FS. The maximum deviation of the return stroke is 0.11821 turns, corresponding to an error of 0.0102%FS. These results indicate that the turn-count accuracy is better than the technical requirement of 1%FS.

The absolute turn count increases monotonically with the number of sampling points, and its overall variation trend remains consistent with that of the reference turn count, without any regression or jump. As can be seen from the local enlarged view at the end position, the absolute turn count at the full-stroke target position is 16191.15039 turns, with a deviation of 48.84961 turns from the reference turn count, corresponding to a full-scale relative error of

0.3008%FS, which satisfies the technical requirements.

The summarized results are listed in Table 3-1

Table 3-1. Summary of Turn-Count Accuracy and Index Compliance under the 25 N·m Condition

Type	Reference Value	Measured Value	Error	Whether≤1%FS
Relative turn count	1160	1160.1228	0.0106%	YES
Absolute turn count	16240	16191.15039	0.3008%	YES
Average zero-return deviation of the scale	0	0.27	0.667%	YES

From Table 5-9, it can be seen that under the 25 N·m load condition, the relative turn count, absolute turn count, and the average relative deviation of the scale zero-return verification all satisfy the technical requirement of ≤ 1%FS.

5. Conclusion

To meet the requirements for stable low-speed operation and accurate turn-count measurement of the permanent magnet synchronous motor used in a logging-while-drilling formation-sampling tool under high-temperature and severe-vibration conditions, an integrated drive-and-control system with the TMS320F28335 as the core was designed and implemented. The system adopts a dual-loop FOC structure, and a fuzzy two-degree-of-freedom PI control strategy based on Mamdani rules is introduced into the speed loop to improve the dynamic response and disturbance rejection capability in the low-speed range. A lead-screw slide experimental platform was established for validation. The results show that, under reciprocating operating conditions, the relative turn count can stably track the reference trajectory, and both the steady-state deviation and the transient deviation during reversal satisfy the requirement of ≤ 1%FS. The cumulative curve of the absolute turn count is monotonic and continuous, without regression or jump, and the terminal relative error is approximately 0.3008%FS, which is consistent with the displacement verification results. These results verify that the proposed scheme possesses good stability and metering reliability under engineering constraints, and can provide a reference for the control and measurement design of logging-while-drilling formation-sampling actuators. Future work may further focus on the calibration of the reduction ratio and screw lead, as well as the optimization of the cross-zero counting strategy during reversal, so as to reduce long-stroke cumulative error and improve the system's adaptability to complex operating conditions.

References

[1] Zhao Xiaoqiang, Liu Shuning, Yang Puhanting, et al. Improved fuzzy adaptive PI control strategy for permanent magnet synchronous motor based on dead-time compensation [J]. Machine Tool & Hydraulics, 2021, 49(08): 8–14.

[2] Zhang Haiyang, Li Jifang, Xiong Junhua, et al. Two-degree-of-freedom PI control of permanent magnet synchronous motor based on extended state observer [J]. Electric Machines & Control Application, 2021, 48(05): 40–45.

[3] Audomsi S, Wattana S, Uthathip N, et al. Development and Design of an Optimal Fuzzy Logic Two Degrees of Freedom-Proportional Integral Derivative Controller for a Two-Area Power System Using the Bee Algorithm[J]. Energies, 2025, 18(4): 915.